Supporting Information

Unveiling the role of cobalt doping for optimizing ammonia electrosynthesis on iron-cobalt oxyhydroxide hollow nanocages

Xinxin Han[a], Cheng Liu[b], Yuan Tang [a], Qiangguo Meng[c], Weizhen Zhou[c], Shixia Chen[*, c], Shuguang Deng[d], Jun Wang[*, c]

[a] School of Resources & Environment, Nanchang University, Nanchang 330031, People's Republic of China

[b] School of Future Technology, Nanchang University, Nanchang 330031, People's Republic of China

[c] School of Chemistry and Chemical Engineering, Nanchang University, Nanchang 330031, People's Republic of China

[d] School for Engineering of Matter, Transport and Energy, Arizona State University, Tempe, AZ 85287, United States

Content

1. Experimental details:

1. 1 Synthesis of Cu_2O nanocubes.

In a typical procedure, 0.75 g $CuSO_4 \cdot 5H_2O$ and 0.294 g sodium citrate were dissolved in 160 mL of deionized water with stirring to form a uniform dispersion. Then, 2 g of NaOH were added to the above solution. Afterwards, 100 mL of 0.03 M ascorbic acid was added to the suspension while stirring for 45 minutes. The resulting mixed solution was aged at room temperature for 1 hour. The precipitate was collected by centrifugation, washed with water and ethanol several times, and then dried in a vacuum at 60 °C overnight.

1.2 Synthesis of FeCoOOH HNCs nanocubes.

The FeCoOOH HNCs with hollow nanocubic structures were prepared according to Pearson's principle by employing Cu_2O nanocubes as starting templates. Specifically, 200 mg of the as-prepared Cu_2O was completely dispersed into a 400 mL mixed solvent of H_2O and ethanol (v/v = 1/1). Then, 13.2 g of PVP (polyvinyl pyrrolidone, Mw = 40000) was dissolved in the solution by ultrasonic treatment for 15 minutes. Subsequently, 100 mg of $FeCl_3 \cdot 6H_2O$ and $CoCl_2 \cdot 6H_2O$ with different molar ratios (1/1, 1/2, and 2/1) were dissolved in this system. After magnetic stirring for 30 minutes, $Na_2S_2O_3$ solution (160 mL, 1 M) was added dropwise into the above mixture while stirring for another 60 minutes. After centrifugation, washing with deionized water and ethanol, and drying in a vacuum at 60 °C for 12 hours, the resulting products were named FeCoOOH HNCs (1/1), FeCoOOH HNCs-H (1/2), and FeCoOOH HNCs-L (2/1).

1.3 Catalyst characterization.

The scanning electron microscopy (SEM) images were obtained using a field emission scanning electron microscopy (FESEM, Hitachi SU8010, Japan). The transmission electron microscopy (TEM) images were collected using a high-resolution TEM (HRTEM, FEI HELIOS NanoLab 600i Titan G2 60-300) and a high-angle annular dark-field scanning TEM (HAADF-STEM, Esprit Super X, Bruker). X-ray photoelectron spectroscopy (XPS) measurements were performed on an ESCALAB 250Xi. Powder X-ray diffraction (XRD) patterns were acquired ussing a Bruker D8 Advance X-ray diffractometer with a Cu Kα radiation (λ=1.5406 Å). The Raman spectra were detected using a Confocal LabRam HR800 spectrometer with 532 nm radiation (HORIBA Jobin Yvon). The textural properties were characterized in a Micromeritics ASAP 2460 apparatus by N_2 adsorption-desorption isotherms at 77 K. UV-Vis measurements were performed using a UV-Vis spectrophotometer (TU-1900, PERSEE). The hydrophobic properties were measured by the Sindatek 100P contact angle goniometer.

1.4 Nitrogen purification

The high purity $^{14}N_2$ and $^{15}N_2$ (Enrichment: 99 atom% ^{15}N) flowed through acid and alkaline solution traps successively to remove the possible NH_3 and NO_x. The purified gas was then passed through a drying tube to prevent vapor before being supplied into the cathodic compartment. The electrolyte obtained from this process was analyzed using spectrophotometric methods to ensure that no NH_3 or NO_x were present.

1.5 Electrochemical measurements.

The electrochemical measurements were performed in a gas-tight H-type cell with three-electrode separated by a proton-exchange membrane (DuPont, Nafion 212). Before testing, the Nafion 212 membrane was pretreated by heating in a 0.5 M H_2SO_4 and 3 wt% H_2O_2 solution at 80 ℃ for 1 hour each, respectively and then putting it into ultrapure water at 80 ℃ for 12 hours. The H-shaped electrochemical cell was also put into ultrapure water at 80 ℃ for 12 hours. All of the NRR electrochemical measurements were performed with a CHI 660E electrochemical workstation (CH Instrument, China) in a three-electrode setup using a platinum plate (Pt,1cm × 1cm) as the counter electrode, Ag/AgCl (saturated KCl solution) as the reference electrode, and FeCoOOH HNCs as the working electrode. All electrochemical measurements were conducted under ambient conditions. The catalyst inks were prepared by dispersing 2 mg catalyst powder into 350 μL of ethanol and 10 μL of Nafion (5 wt%) and 140 μL of ultrapure water under ultrasonication for 1 hour, and then dropping 50 μL of the catalyst inks on carbon paper with 1×1 cm^2 used as the working electrode. The polarization curves were measured with a scan rate of 5.0 mV s^{-1} at ambient conditions. Before the NRR measurements, the N_2 (99.99%) feeding gas was first purged to eliminate the potential NO_x and NH_3 contaminants. The electrolyte was also bubbled with high-purity N_2, which was purged for 30 minutes to expel the air. In this study, all measured potential (vs. Ag/AgCl) were transformed into the potentials vs. the reversible hydrogen electrode (RHE) via calibration with the following equation: E (vs RHE) = E (vs Ag/AgCl) + 0.197 + 0.059×pH.

1.6 Determination of NH_3.

Concentration of produced NH_3 in 0.1 M Na_2SO_4 was determined by indophenol blue method. In detail, 4 mL of post-tested solution was removed from the cathodic cell, and then added to 50 μL of oxidizing solution (sodium hypochlorite (ρ_{Cl} = 4~4.9) and 0.75 M sodium sodium hydroxide), 500 μL of coloring solution (0.4 M sodium salicylate and 0.32 M sodium hydroxide) and 50 μL of catalyst solution (0.5 g $Na_2[Fe(CN)_5NO]\cdot 2H_2O$ diluted to 50 mL with deionized water). After standing in darkness at room temperature for 2 hours, the UV-Vis absorption spectrum was measured at a wavelength of 655 nm. The concentration-absorbance curves were calibrated using standard NH_4Cl solution with a serious of concentrations (0.0, 0.1, 0.2, 0.3, 0.4, 0.5 μg mL^{-1} in 0.1 M Na_2SO_4 solution). The standard curve (Y = 0.4497X + 0.0278, R^2 = 0.9999) showed good linear relation of absorbance value with NH_3 concentration in 0.1 M Na_2SO_4 in three independent calibrations.

1.7 Determination of N_2H_4.

The N_2H_4 presented in the electrolyte was estimated by the Watt and Chrisp method. A mixture solution of $C_9H_{11}NO$ (2g), concentrated HCl (10 mL) and ethanol (100 mL) was used as a color regent. Specifically, 5 mL of electrolyte from the cathodic chamber after 2 hours of electrochemical test was added to 5 mL of the as-prepared color reagent and stirred for 15 minutes at room temperature. Then, the UV-Vis absorption spectrum was measured at a wavelength of 455 nm. The concentration-absorbance curves were calibrated using standard $N_2H_4\cdot H_2O$ solution with a series of N_2H_4 concentrations (0.0, 0.1, 0.2, 0.3, 0.4, 0.5 μg mL^{-1} in 0.1 M Na_2SO_4 solution). The standard curve (Y=0.7083

X + 0.0216, R^2=0.9999) showed good linear relationship of absorbance value with N_2H_4 concentration in 0.1 M Na_2SO_4, as confirmed by three independent calibrations.

1.8 Determination of NO_x.

NO_x was determined using N-(1-naphthyl) ethylenediamine dihydrochloride spectrophotometric methods with some modification. Specifically, 0.5 g sulfanilic acid was dissolved in 90 mL H_2O and 5 mL acetic acid. Then, 5 mg N-(1-naphthyl)-ethylenediamine dihydrochloride was added and the solution was filled to 100 mL to obtain the chromogenic agent. One milliliter of the treated electrolyte was mixed with 4 mL of the chromogenic agent and left in darkness for 15 minutes. The UV-Vis absorption spectrum was then measured at 540 nm. The concentration-absorbance curves were calibrated using standard sodium nitrite solution with a series of concentrations (0.0, 0.5, 1, 1.5, 2, 2.5 μg mL^{-1} in 0.1 M Na_2SO_4 solution). The standard curve (Y = 0.1314 X + 0.005, R^2 = 0.9998) shows good linear relation of absorbance value with NOx concentration in 0.1 M Na_2SO_4, as determined by three independent calibrations.

1.9 ^{15}N isotopic labeling experiment.

Before NRR measurements, $^{15}N_2$ was pre-purified, and the electrolyte was also bubbled with high-purity $^{15}N_2$, which is purged for 30 minutes to expel the air. After electrolysis for 2 hours, all the electrolyte (50 ml) in cathode chamber was removed, and its pH was adjusted to 3-4 by adding concentrated H_2SO_4 solution. The solution was then evaporated under low vacuum at 30 ℃ until it became 1 mL. Next 250 μL of electrolyte was mixed with 150 μL of D_2O, 50 μL of 3.5 mg mL^{-1} MA solution and 50

μL of 0.05 M H_2SO_4 to obtain 0.5 mL. The produced ammonia was quantified using ^1H nuclear magnetic resonance (NMR) measurements. Maleic acid (MA) was used for quantitative analysis.

1.10 Calculations of NH_3 yield rate and Faradaic efficiency.

The equation of NH_3 yield rate is:

$$R = \frac{C \times V}{m \times t}$$

The equation of Faradaic efficienency is:

$$FE = \frac{3F \times C \times V}{17 \times Q} \times 10^{-6} \times 100\%$$

In these equations, **R** (μg h^{-1} mg-1 cat) is the NH_3 yield, **C** (μg mL^{-1}) is the measured NH_3 concentration, **V** (mL) is the volume of the electrolyte (in our work 50 mL), **F** (96485.34 C mol^{-1}) is the Faradaic constant, **m** (mg) was the loading mass of the catalysts, **t** (h) is the reaction time, **Q** (C) is the total charge during the NRR.

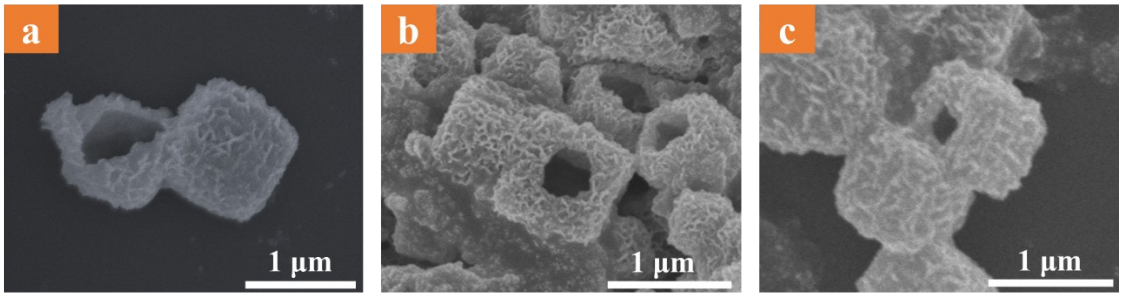

Figure S1. The SEM image of (a) FeCoOOH HNCs, (b) FeCoOOH HNCs-L, and (c) FeCoOOH HNCs-H.

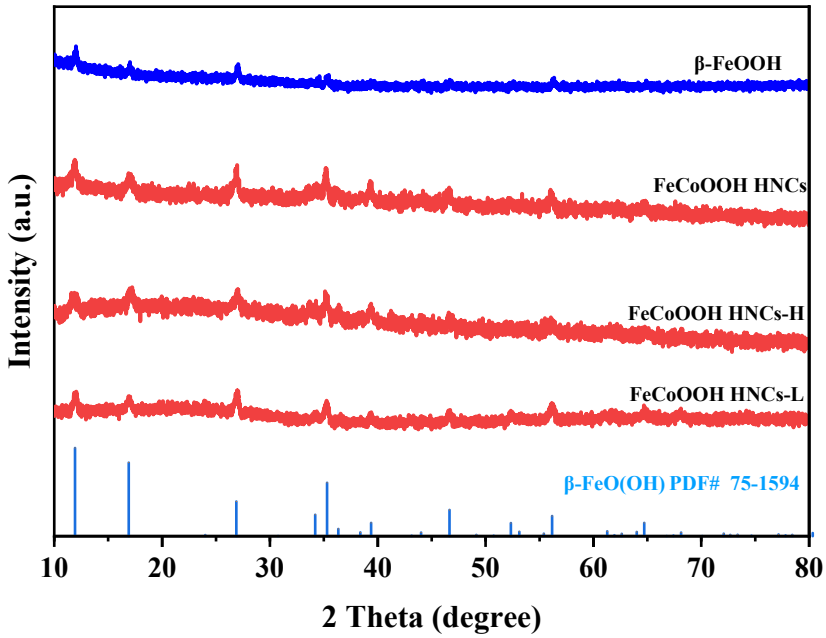

Figure S2. PXRD patterns of the *β*-FeOOH, FeCoOOH HNCs, FeCoOOH HNCs-H, and FeCoOOH HNCs-L samples.

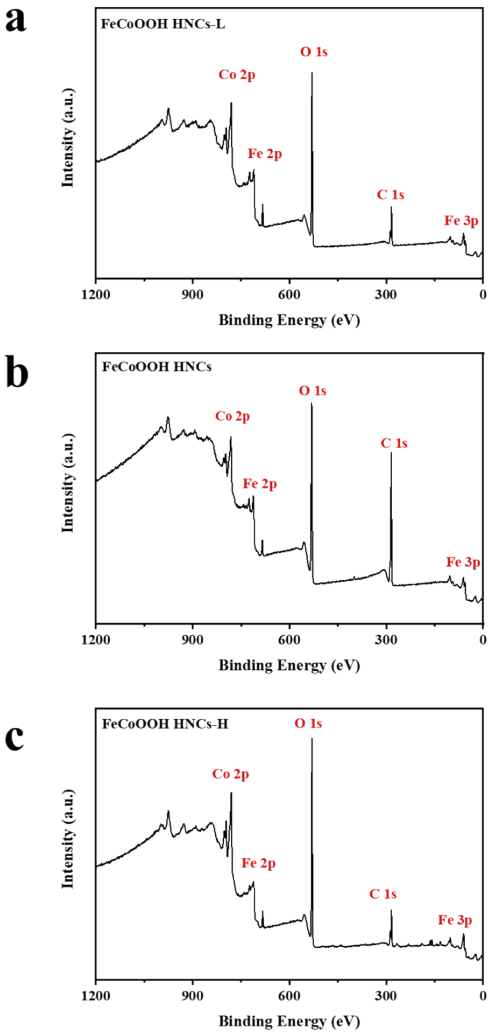

Figure S3. Wide XPS survey spectrum for (a) FeCoOOH HNCs-L, (b) FeCoOOH HNCs, and (c) FeCoOOH HNCs-H.

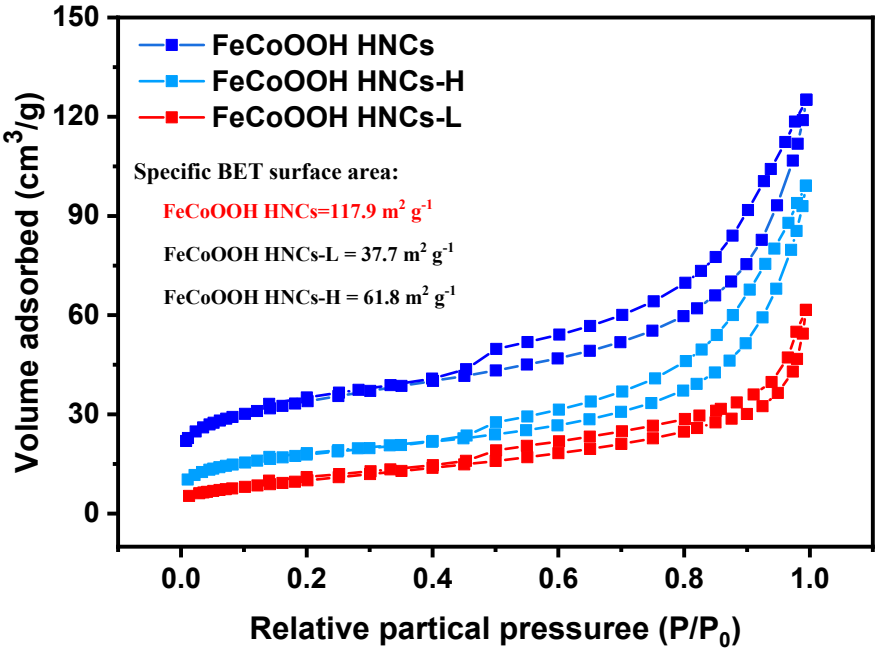

Figure S4. N_2 adsorption-desorption isotherms of the FeCoOOH HNCs, FeCoOOH HNCs-H, and FeCoOOH HNCs-L at 77 K.

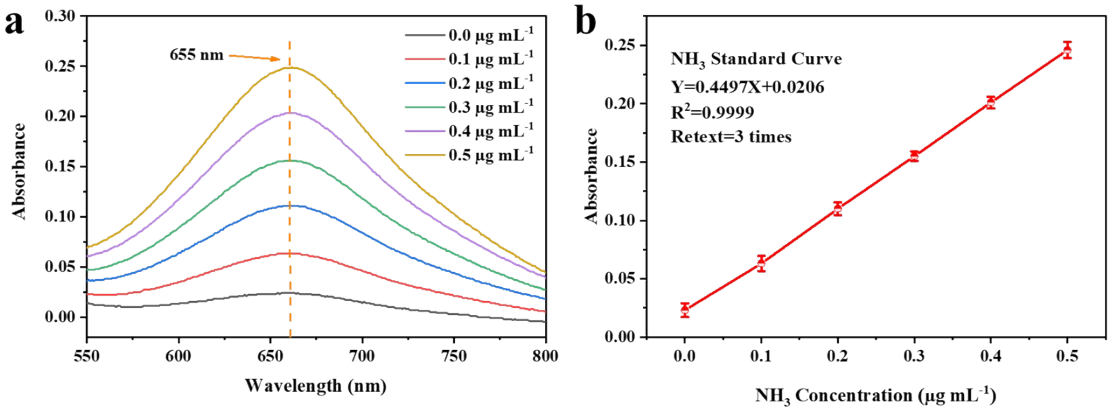

1

2 **Figure S5.** (a) UV-Vis absorption spectra of indophenol assays with NH_3 in 0.1 M

3 Na_2SO_4 after standing in darkness for 2 h at room temperature; (b) Calibration curve

4 used for calculation of NH_3 concentration.

5

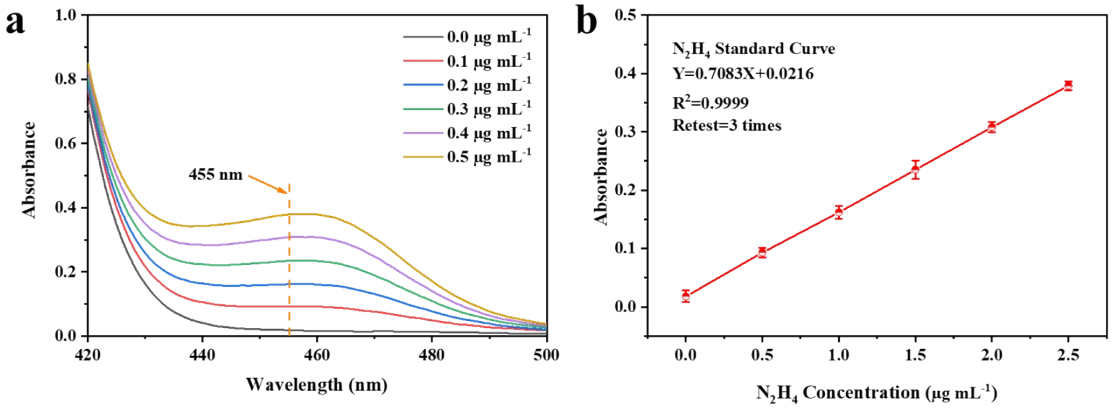

1

2 **Figure S6.** (a) UV-Vis absorption spectra of various $N_2H_4 \cdot H_2O$ concentrations after

3 incubation for 15 min at room temperature; (b) Calibration curve used for calculation

4 of N_2H_4 concentration.

5

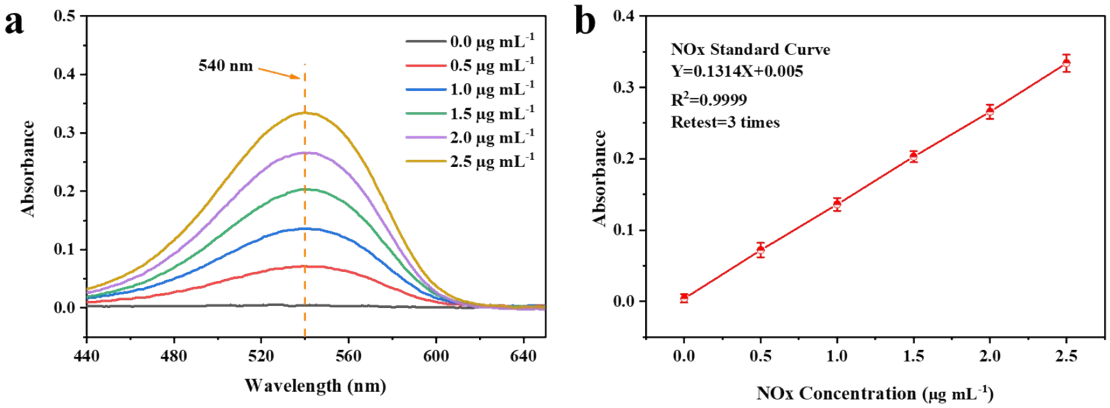

Figure S7. (a) UV-Vis absorption spectra of various NO_x concentrations after standing in darkness for 15 min at room temperature; (b) Calibration curve used for calculation of NOx concentration.

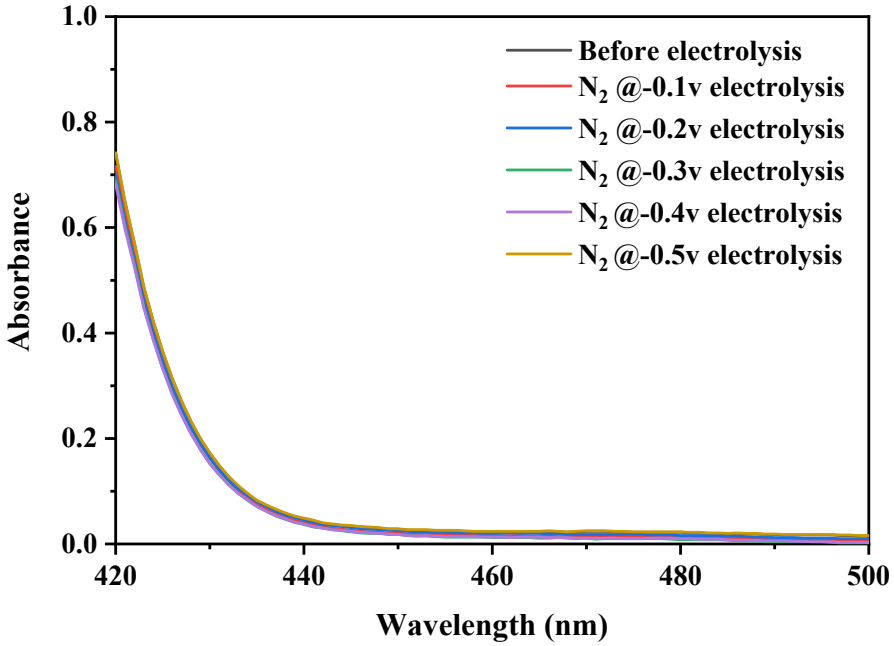

Figure S8. UV-Vis absorption spectra of the electrolytes stained with indicator after electrolysis at different potentials under N_2 atmosphere for 2 h by using the Watt and Chrisp method.

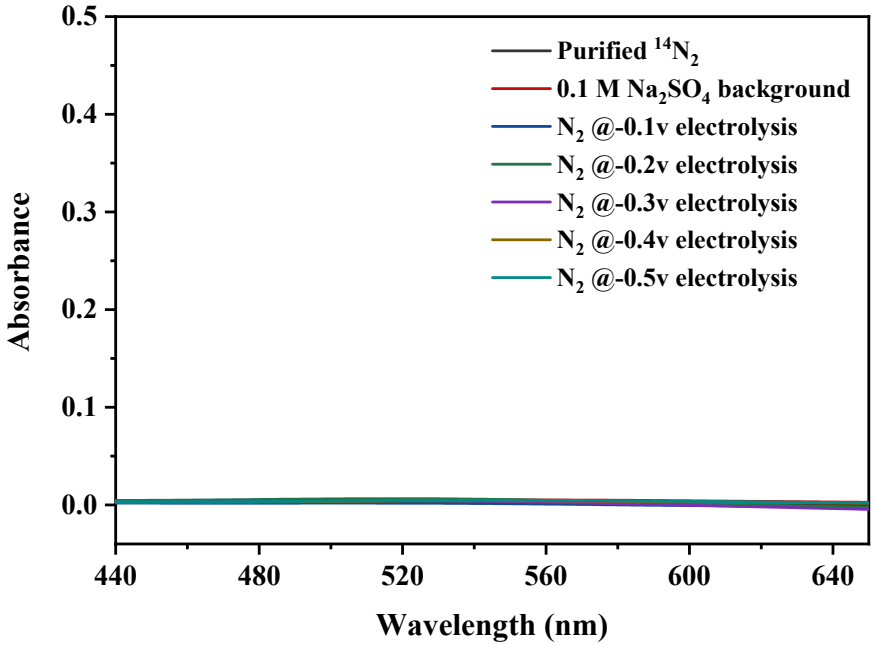

Figure S9. UV-Vis absorption spectra of the electrolytes stained with indicator after electrolysis at different potentials under N_2 atmosphere for 2 h by using N-(-1-naphthyl) ethylenediamine dihydrochloride spectrophotometric method.

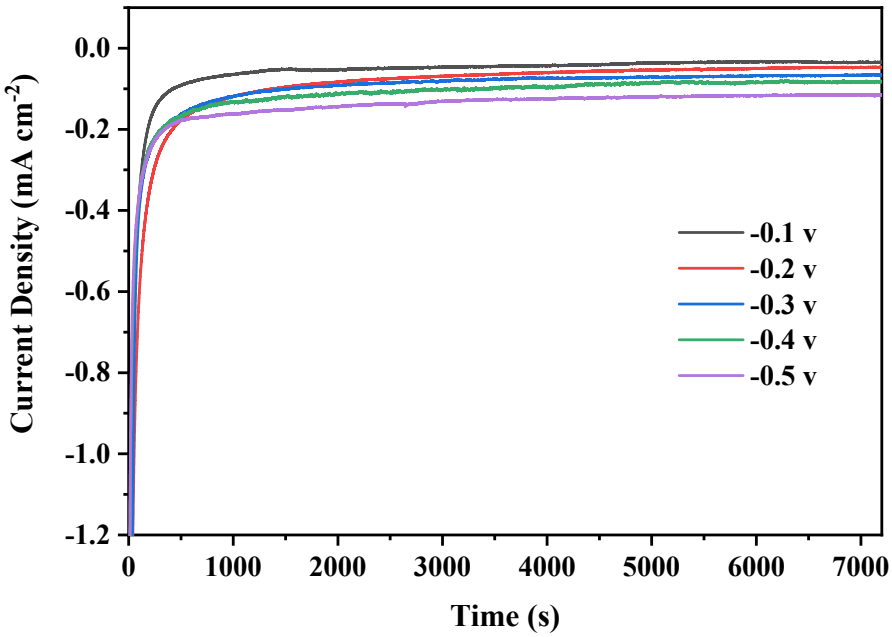

Figure S10. Chronoamperometry results for the FeCoOOH HNCs at different potentials for 2 h.

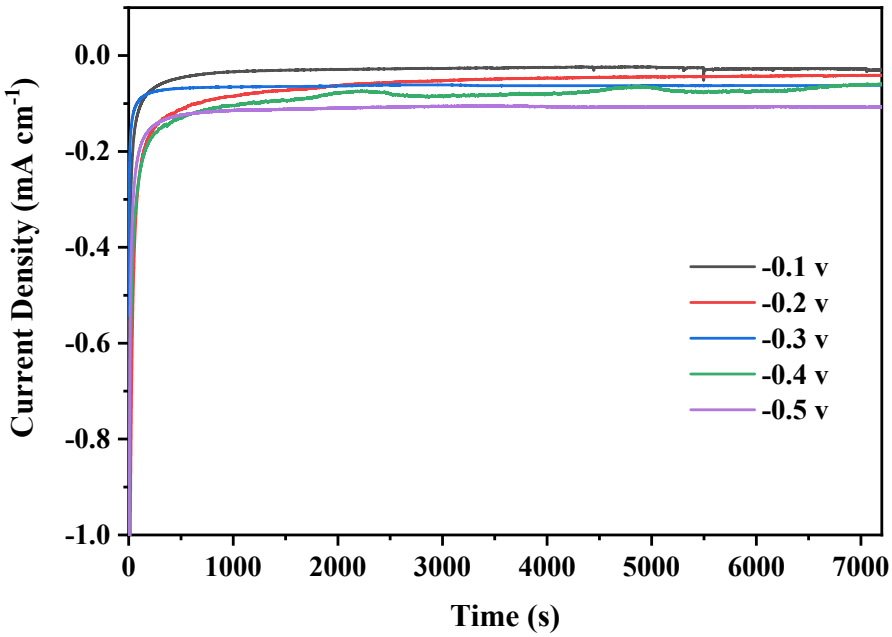

Figure S11. Chronoamperometry results for the FeCoOOH HNCs-H at different potentials for 2 h.

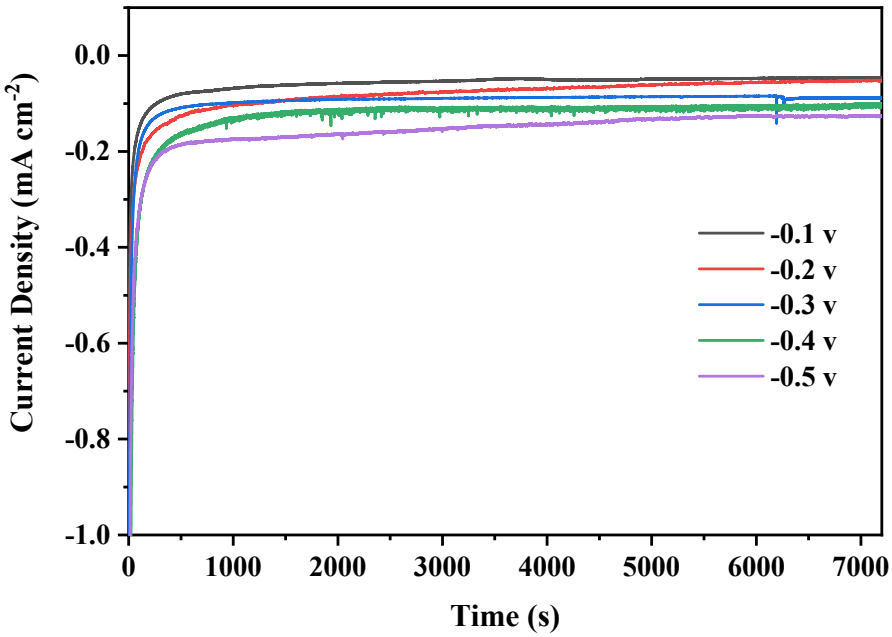

Figure S12. Chronoamperometry results for the FeCoOOH HNCs-L at different potentials for 2 h.

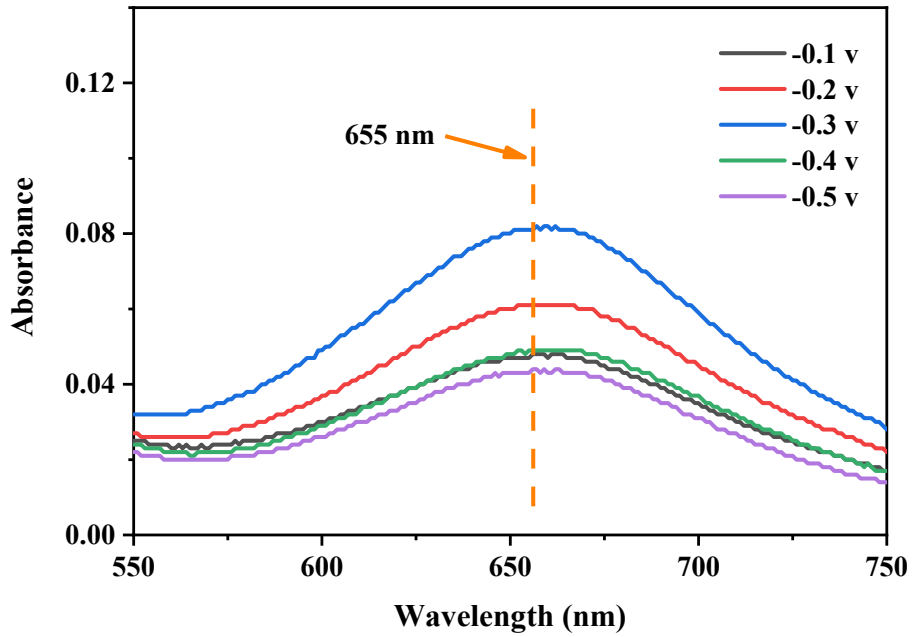

Figure S13. UV-Vis absorption spectra of the electrolytes stained with indophenol indicator after NRR electrolysis by FeCoOOH HNCs catalyst at different potentials for 2 h.

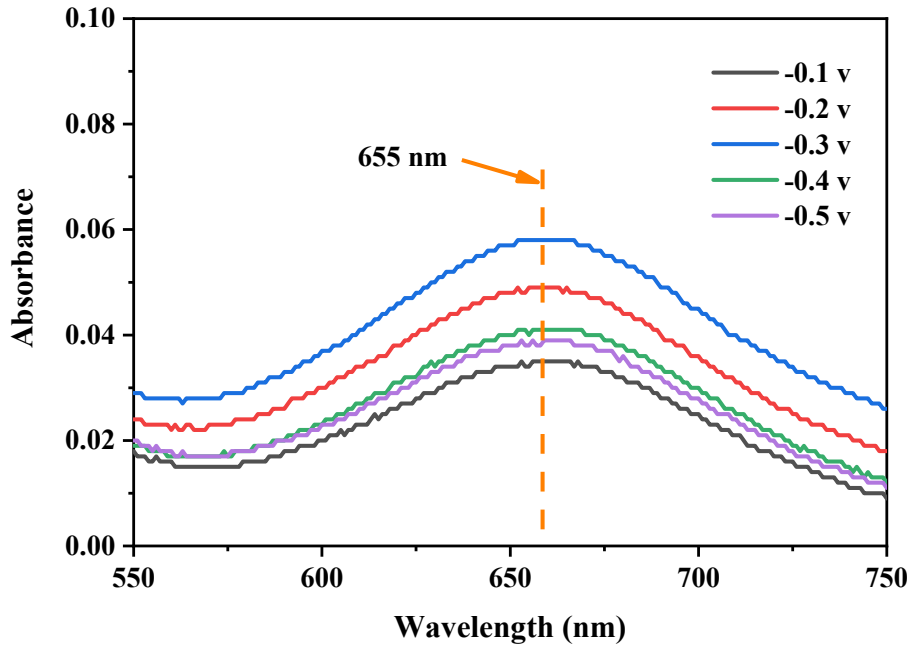

Figure S14. UV-Vis absorption spectra of the electrolytes stained with indophenol indicator after NRR electrolysis by FeCoOOH HNCs-H catalyst at different potentials for 2 h.

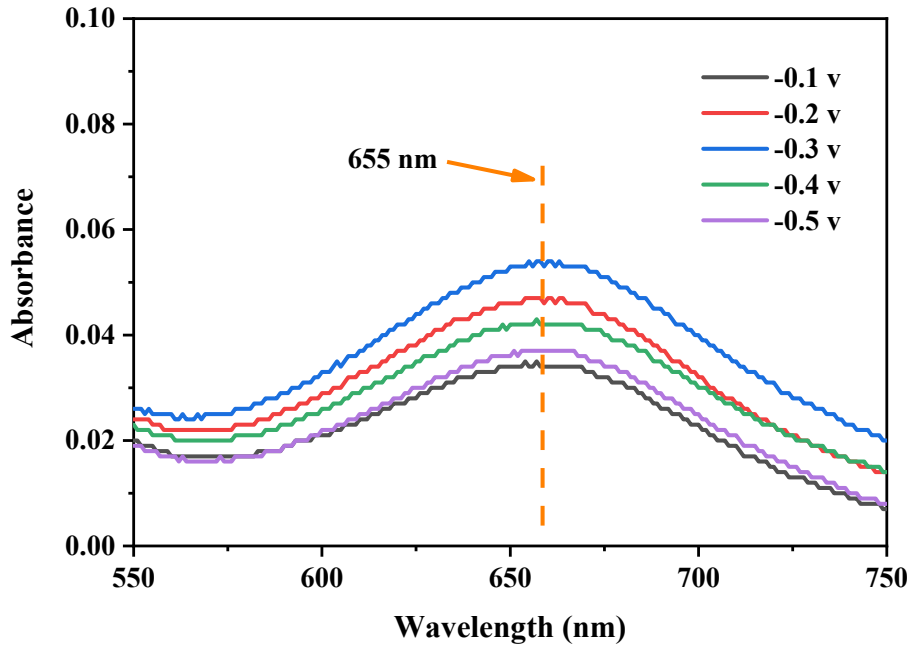

Figure S15. UV-Vis absorption spectra of the electrolytes stained with indophenol indicator after NRR electrolysis by FeCoOOH HNCs-L catalyst at different potentials for 2 h.

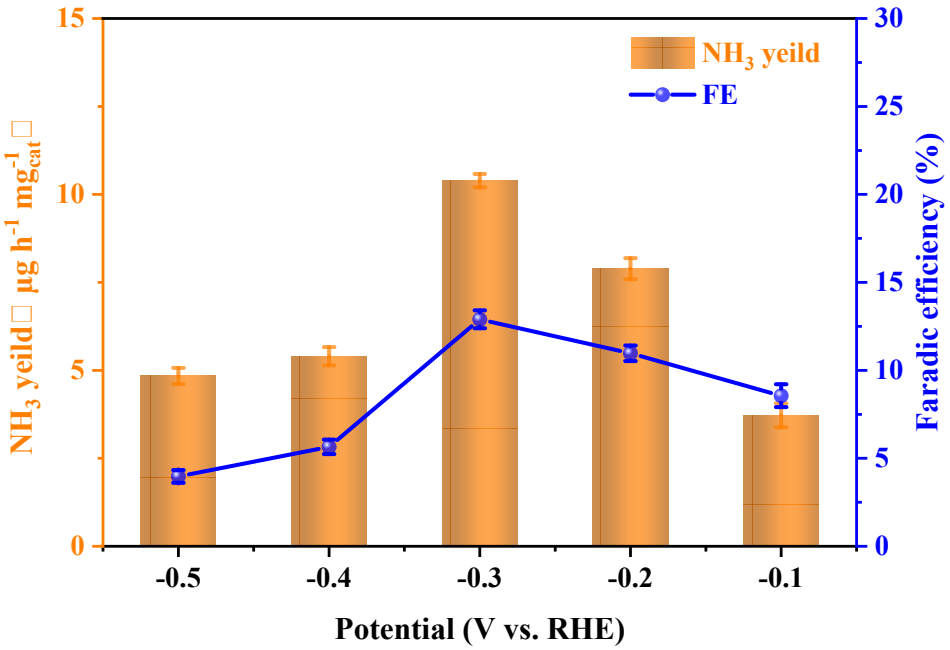

Figure S16. NH_3 yield rate and FE for FeCoOOH HNCs-H catalyst at different potentials for 2 h NRR measurement.

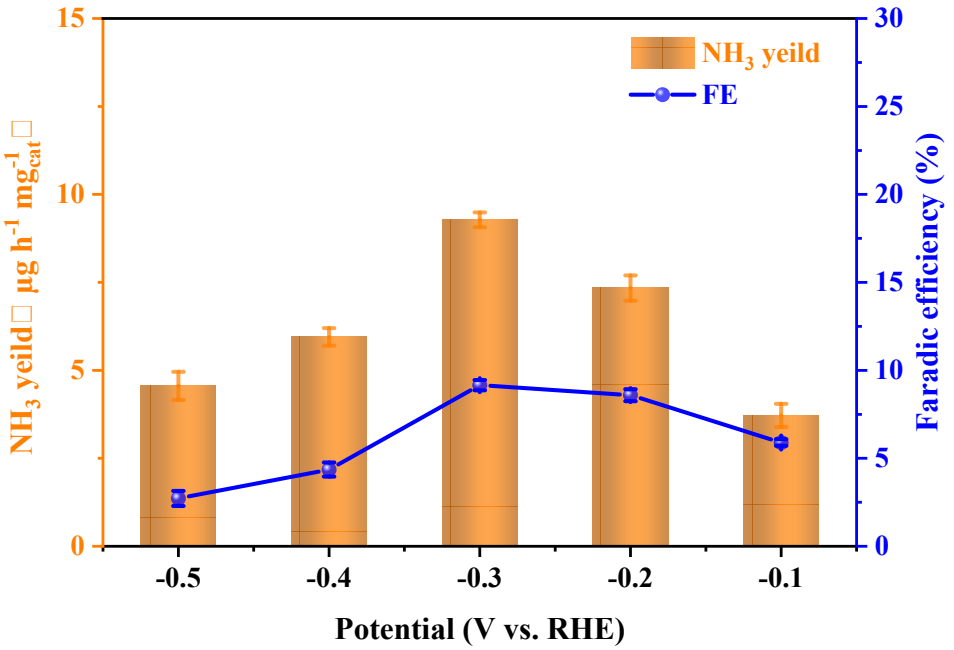

Figure S17. NH_3 yield rate and FE for FeCoOOH HNCs-L catalyst at different potentials for 2 h NRR measurement.

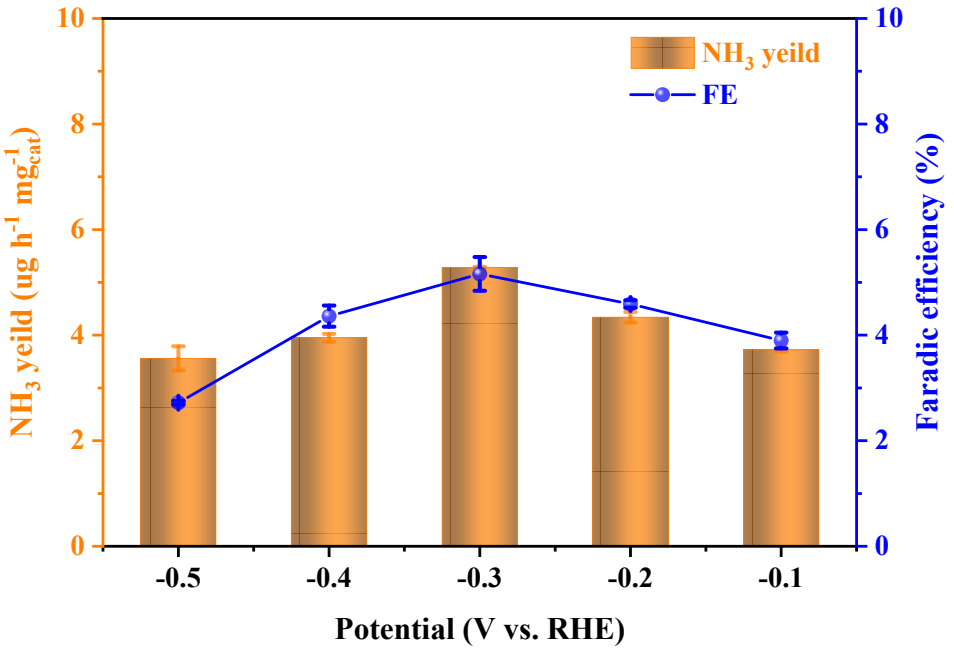

Figure S18. NH_3 yield rate and FE for β-FeOOH catalyst at different potentials for 2 h NRR measurement.

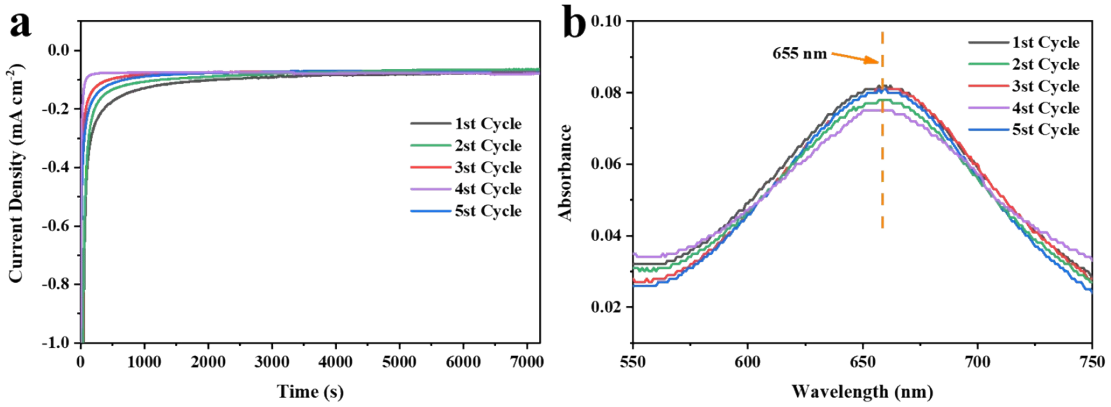

Figure S19. (a) The chronoamperometry assessment and (b) the UV-Vis absorption spectra of FeCoOOH HNCs catalyst electrolyzed at -0.3 V for 5 cycles.

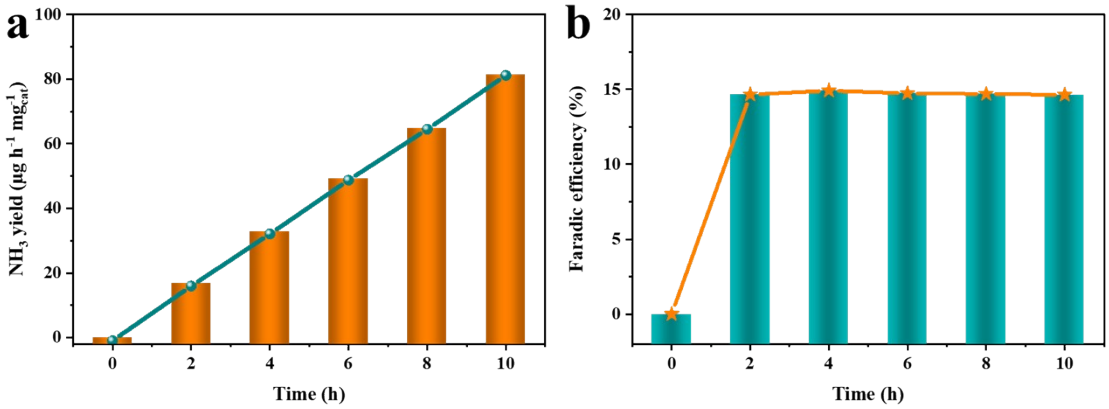

Figure S20. (a) The quantity of NH_3 with various electrolysis times and (b) NH_3 FE at various electrolysis times using FeCoOOH HNCs at -0.3 V.

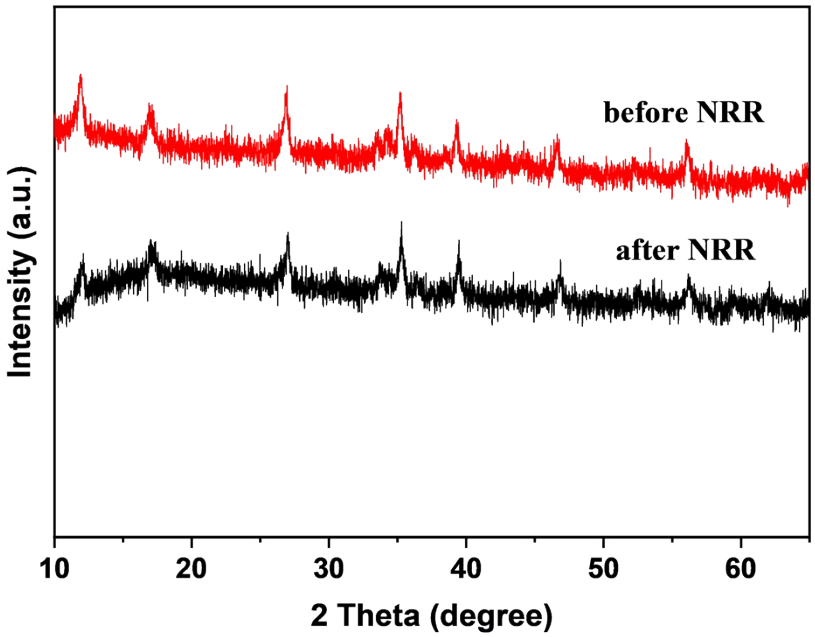

Figure S21. XRD patterns of FeCoOOH HNCs catalyst after long-term NRR test.

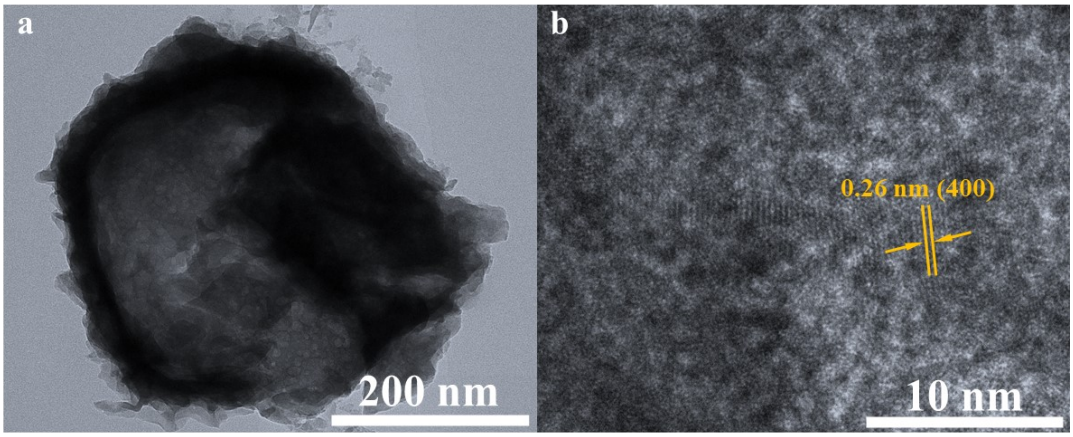

Figure S22. TEM image of FeCoOOH HNCs catalyst after long-term NRR test.

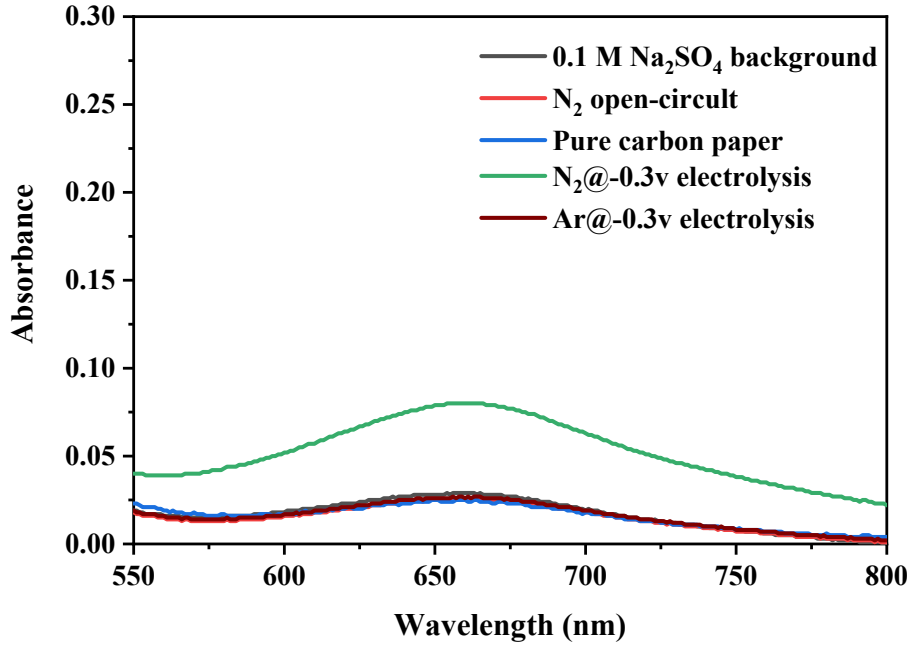

Figure S23. UV-vis absorption spectra of different samples in control experiments to eliminate possible environmental influences.

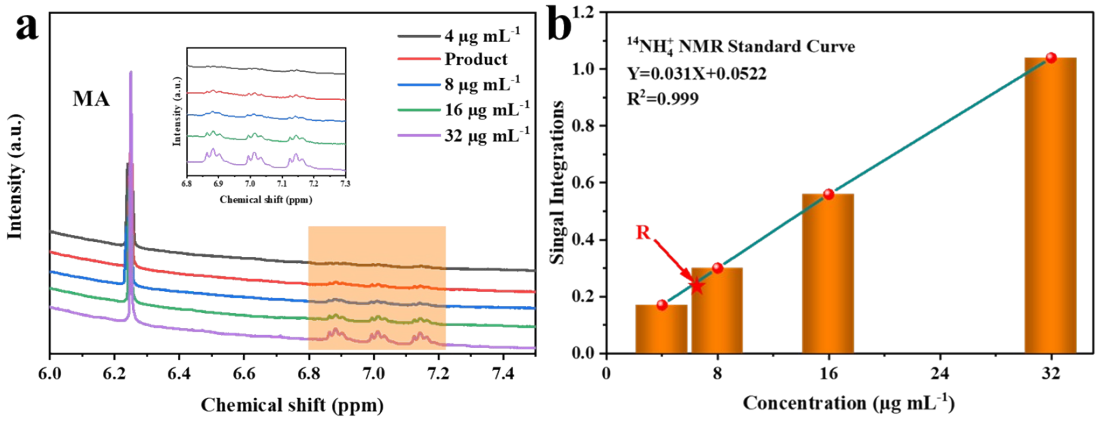

Figure S24. (a) The ^{1}H NMR (400 MHz) spectra of a series of $^{14}NH_4^+$ standard solutions with known concentrations and the FeCoOOH HNCs catalyst produced $^{14}NH_4^+$. Maleic acid (MA) is used as the internal standard; (b) the corresponding calibration curve is used for the calculation of NH_4^+ concentration.

The experiment contained several steps, including the preparation of standard solutions and the measurement of NH_3 concentrations produced by FeCoOOH HNCs catalyst. First, $(^{14}NH_4)_2SO_4$ solution was used to prepare different concentrations (8, 16, 32, 64 μg mL^{-1}) of $^{14}NH^{4+}$ standard solutions using 0.1 M Na_2SO_4 as the solvent. Next, a 3.5 mg mL^{-1} MA solution was prepared using D_2O as the solvent. In the third step, 250 μL of $^{14}NH^{4+}$ standard solution was mixed with 150 μL of D_2O, 50 μL of MA solution, and 50 μL of 0.05 M H_2SO_4 to obtain different concentrations (4, 8, 16, and 32 μg mL^{-1}) of $^{14}NH^{4+}$ standard solution for ^{1}H NMR measurement. After 2 h of electrocatalysis, 50 mL of the cathode's electrolyte was combined with 50 μL of 0.05 M H_2SO_4 to prevent the loss of $^{14}NH^{4+}$. The remaining electrolyte was then spun into the rotary evaporator and reduced to 1 mL. Next, 250 μL of electrolyte was mixed with 150 μL of D_2O, 50 μL of MA solution, and 50 μL of 0.05 M H_2SO_4 to obtain the product of NH_3 as R(NH_3). The fifth step involved performing ^{1}H NMR measurement on Bruker

NMR 400 MHz with 500 scans. The integral areas of MA in the series of $^{14}NH_4^+$ standard solutions were normalized to 1.00 to obtain the integral areas of $1^{14}NH_4^+$ standard solutions and R(NH^3), which were 0.17, 0.3, 0.56, 1.04, and 0.25. A calibration curve was plotted using normalized $^{14}NH_4^+$ integral area versus concentration. According to the calibration curve, the NH_3 concentration produced by FeCoOOH HNCs catalyst was 6.38 μg mL^{-1} for 1 mL electrolyte after enrichment program. Therefore, 6.38 μg NH_3 was produced in the original electrolyte for 2 h catalysis reaction. Considering the catalyst's loading mass was 0.2 mg, the NH_3 yield rate was calculated to be 16.0 $\mu g \cdot h^{-1} \cdot mg_{cat}^{-1}$, which was consistent with the result determined by the indophenol blue method.

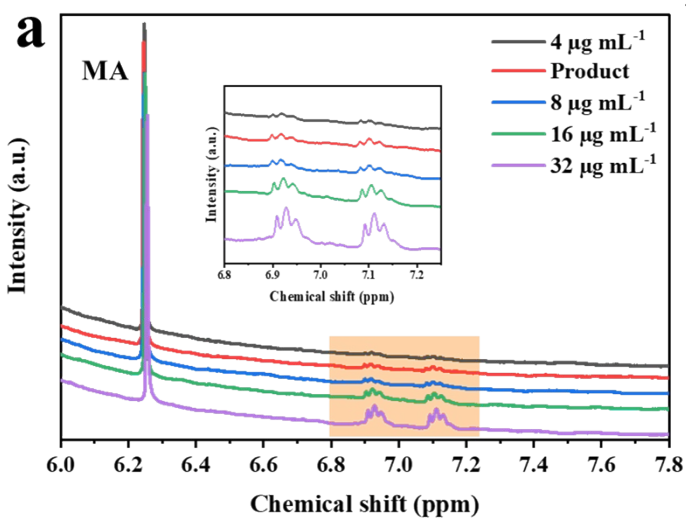

Figure S25. (a) The ^{1}H NMR (400 MHz) spectra of a series of $^{15}NH_4^+$ standard solutions with known concentrations and the FeCoOOH HNCs catalyst produced $^{15}NH_4^+$. Maleic acid (MA) is used as the internal stand; (b) The corresponding calibration curve is used for the calculation of NH_4^+ concentration.

The specific steps of the experiment are the same as **Figure S24** but using $(^{15}NH_4)_2SO_4$ solution and $^{15}N_2$. The obtained integral areas of $^{15}NH_4^+$ standard solutions and R(NH_3) were 0.09, 0.19, 0.45, 0.92 and 0.16. According to the calibration curve, the concentration of NH_3 produced by FeCoOOH HNCs catalyst was 6.57 μg mL^{-1} for 1 mL electrolyte after enrichment program. Then 6.57 μg NH_3 was produced in 50 mL original electrolyte for 2 h catalysis reaction. Considering the loading mass of catalyst is 0.2 mg, so the NH_3 yield rate was calculated to be 16.4 μg·h^{-1}·mg-1 cat, which agreed with the result determined by the indophenol blue method and ^{1}H NMR measurements for $^{14}NH_4^+$.

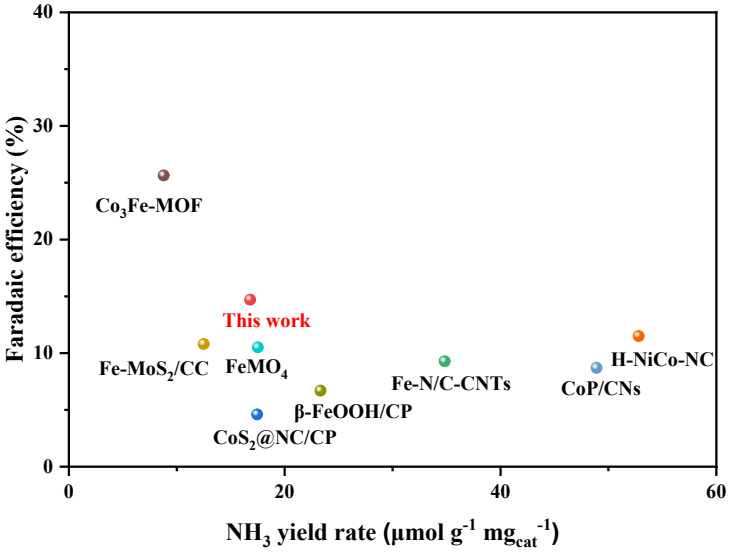

Figure S26. NH_3 yield rate and FE of FeCoOOH HNCs in comparison with reported NRR electrocatalysts;

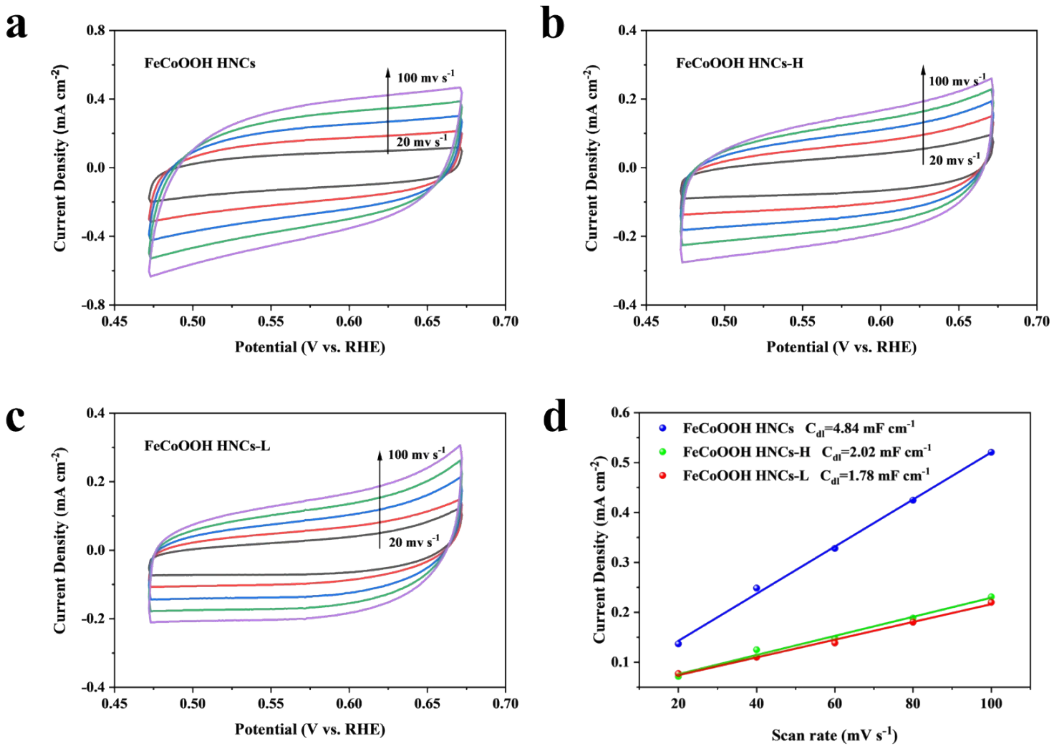

Figure S27. (a-c) Cyclic voltammetry curves of Fe_xCo_xOOH HNCs (1:1, 1:2, and 2:1) at various scan rates (20 mV s^{-1} to 100 mV s^{-1}); (d) Current density *vs* scan rate of as-prepared samples and the corresponding linear slopes.

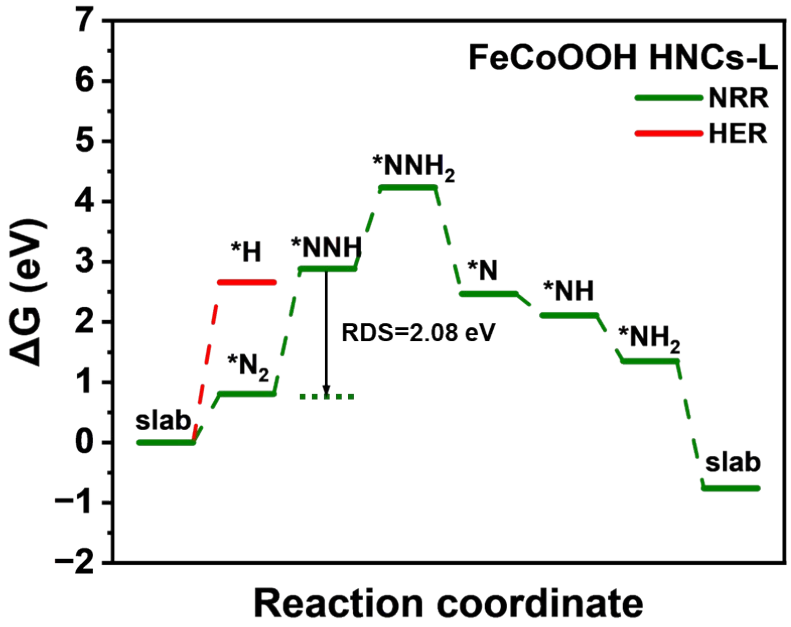

1

2 **Figure S28.** The free energy landscapes and optimized structures of various

3 intermediates along the reaction path on FeCoOOH HNCs-L reaction units.

4

5

6

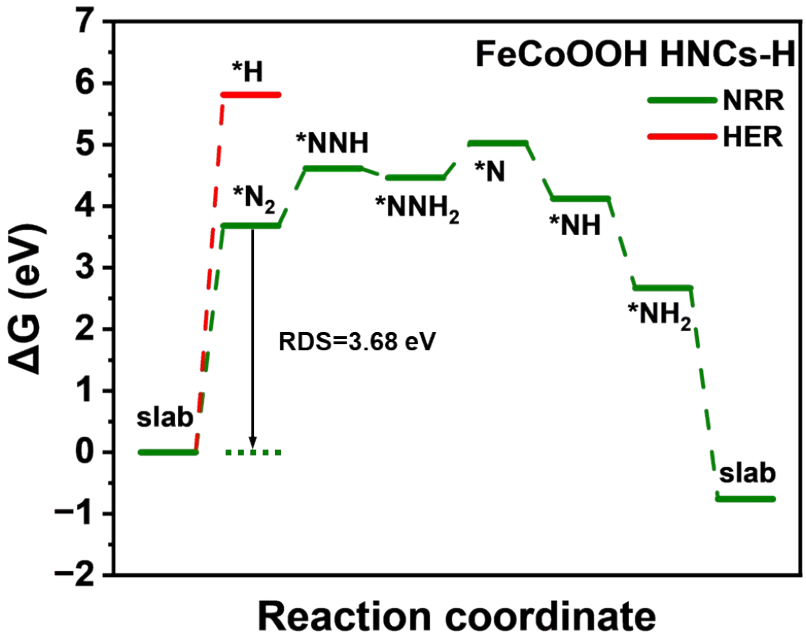

1

2 **Figure S29.** The free energy landscapes and optimized structures of various

3 intermediates along the reaction path on FeCoOOH HNCs-H reaction units.

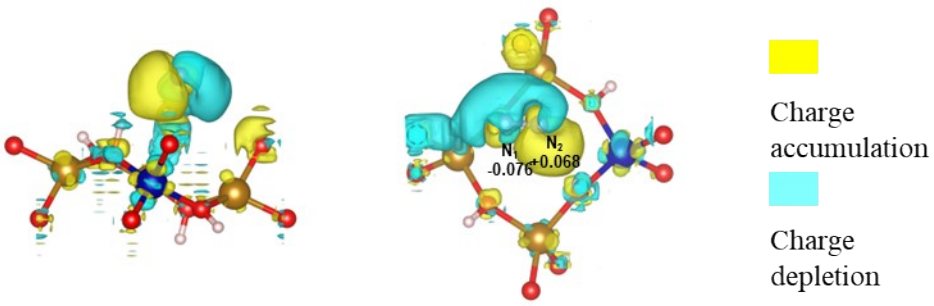

Figure S30. Charge density difference image of *N_2 absorbed on FeCoOOH HNCs-L surface.

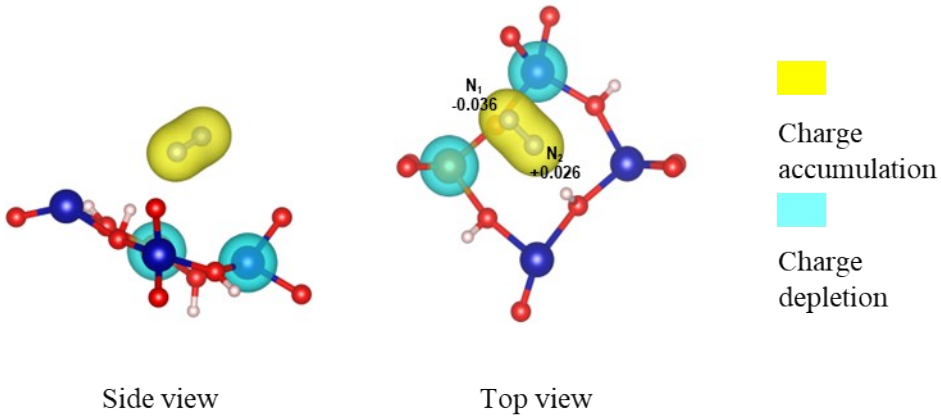

Figure S31. Charge density difference image of *N_2 absorbed on FeCoOOH HNCs-H surface.

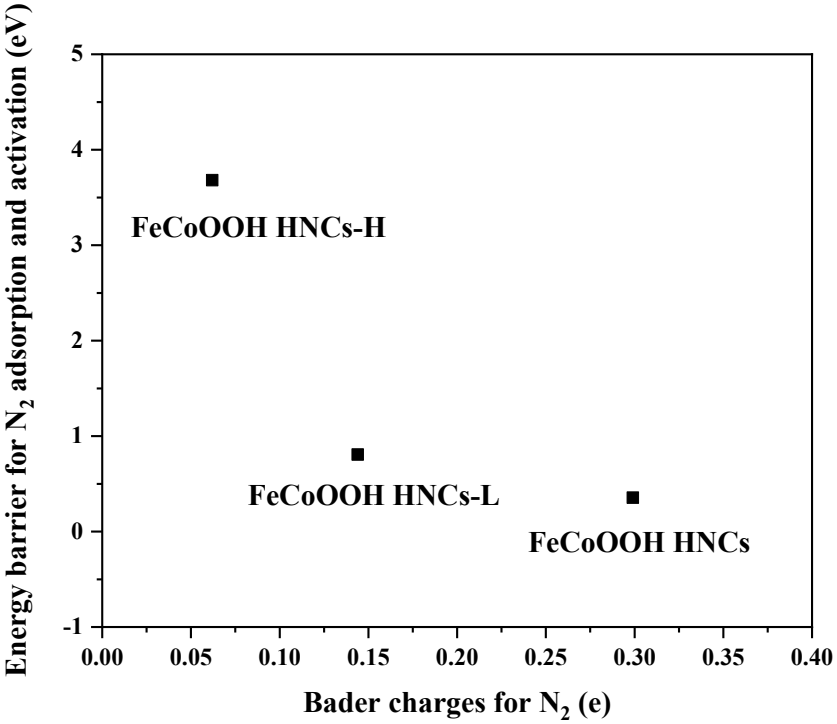

Figure S32. Bader charges for N_2 of FeCoOOH HNCs-L, FeCoOOH HNCSs and FeCoOOH HNCs-H.

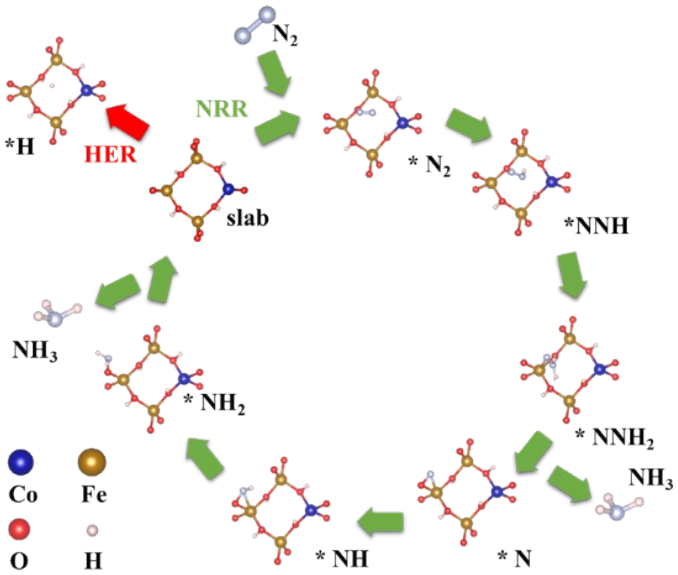

Figure S33. The free energy landscapes and optimized structures of various intermediates along the reaction path on FeCoOOH HNCs-L.

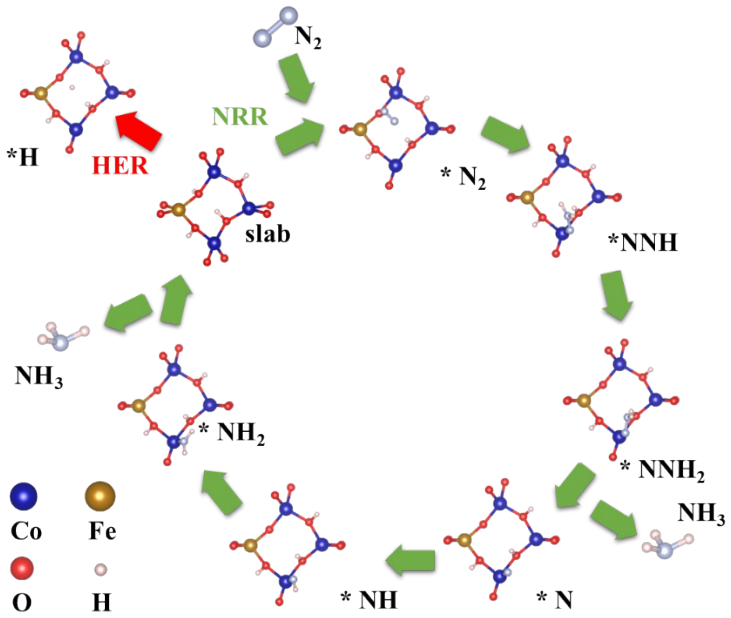

Figure S34. The free energy landscapes and optimized structures of various intermediates along the reaction path on FeCoOOH HNCs-H.

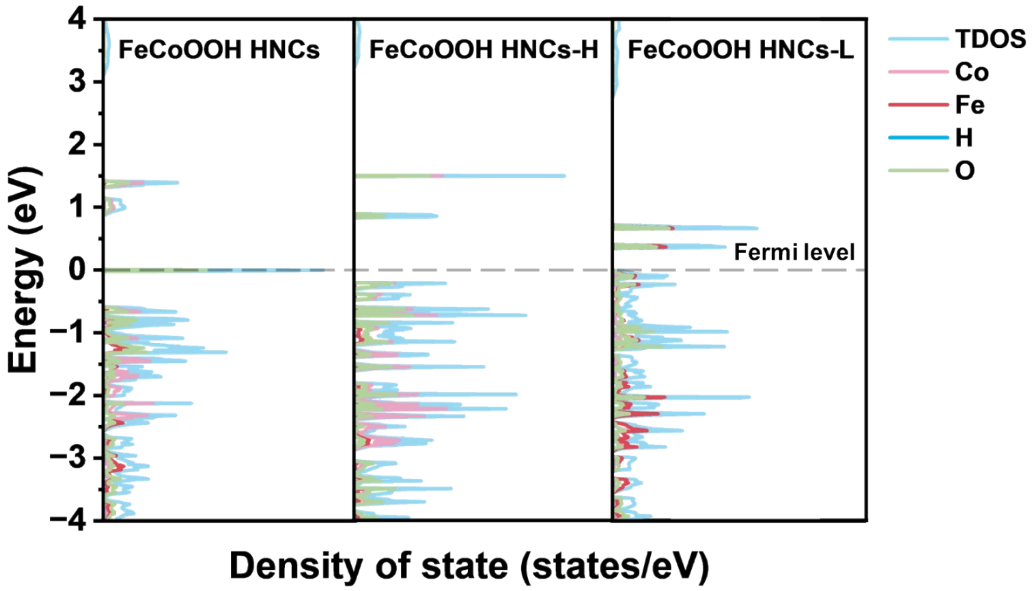

Figure S35. PDOS of the three reaction sites; the Fermi level is set as the energy zero point.

3. Tables

Table S1. ICP results of the FeCoOOH HNCs

Catalysts	Fe/Co (mol%)
FeCoOOH HNCs	1:1.11
FeCoOOH HNCs-H	1:2.14
FeCoOOH HNCs-L	1.94:1

1 Table S2. The comparable table of state-of-the-art NRR catalysts.

Catalyst	System	NH_3 yield rate	FE (%)	References
FeCoOOH HNCs	0.1 M Na_2SO_4	16.8 μg h^{-1} mg-1 cat (0.2 mg)	14.7	This work
CoS_2@NC/CP	0.1 M HCl	17.45 μg h^{-1} mg-1 cat (0.1 mg)	4.6	[1]
Fe-N/C-CNTs	0.1 M KOH	34.83 μg h^{-1} mg-1 cat (0.1mg)	9.28	[2]
Co-$FePS_3$ nanosheets	0.1 M KOH	90.6 μg h^{-1} mg-1 cat (0.04 mg)	3.38	[3]
Fe-MoS_2/CC	0.1 M KOH	12.5 μg h^{-1} cm^{-2}	10.8	[4]
$FeMO_4$	0.1 M Na_2SO_4	17.51 μg h^{-1} mg-1 cat (0.38 mg)	10.5	[5]
CoVP@NiFeV	0.05 M H_2SO_4	1.6 × 10^{-6} mol h^{-1} cm^{-2}	13.8	[6]
Co_3Fe-MOF	1.0 M KOH	8.79μg h^{-1} mg-1 cat	25.64	[7]
β-FeOOH/CP	0.5 M $LiClO_4$	23.32 μg h^{-1} mg-1 cat	6.7	[8]
H-NiCo-NC	0.1 M Na_2SO_4	52.8 μg h^{-1} mg-1 cat	11.5	[9]
CoP/CNs	0.1 M Na_2SO_4	48.9 μg h^{-1} mg-1 cat	8.7	[10]

VFe/NC	0.1 M KOH	73.44 μg h^{-1} mg-1 cat	43	[11]

1

References

1 P. Wei, H. Xie, X. Zhu, R. Zhao, L. Ji, X. Tong, Y. Luo, G. Cui, Z. Wang and X. Sun, *ACS Sustain. Chem. Eng.*, 2020, **8**, 29–33.

2 Y. Wang, X. Cui, J. Zhao, G. Jia, L. Gu, Q. Zhang, L. Meng, Z. Shi, L. Zheng, C. Wang, Z. Zhang and W. Zheng, *ACS Catal.*, 2019, **9**, 336–344.

3 H. Huang, F. Li, Q. Xue, Y. Zhang, S. Yin and Y. Chen, *Small*, 2019, **15**, 1903500.

4 X. Zhao, X. Zhang, Z. Xue, W. Chen, Z. Zhou and T. Mu, *J. Mater. Chem. A*, 2019, **7**, 27417–27422.

5 J. Wu, Z. X. Wang, S. Li, S. Niu, Y. Zhang, J. Hu, J. Zhao, P. Xu and P. Xu, *Chem. Commun.*, 2020, **56**, 6834–6837.

6 M. Arif, G. Yasin, L. Luo, W. Ye, M. A. Mushtaq, X. Fang, X. Xiang, S. Ji and D. Yan, *Appl. Catal. B Environ.*, 2020, **265**, 118559.

7 W. Li, W. Fang, C. Wu, K. N. Dinh, H. Ren, L. Zhao, C. Liu and Q. Yan, *J. Mater. Chem. A*, 2020, **8**, 3658–3666.

8 X. Zhu, Z. Liu, Q. Liu, Y. Luo, X. Shi, A. M. Asiri, Y. Wu and X. Sun, *Chem. Commun.*, 2018, **54**, 11332–11335.

9 Z. Zou, L. Wu, F. Yang, C. Cao, Q. Meng, J. Luo, W. Zhou, Z. Tong, J. Chen, S. Chen, S. Zhou, J. Wang and S. Deng, *ChemSusChem*, 2022, **15**, e202200127.

10 S. Zhang, W. Gong, Y. Lv, H. Wang, M. Han, G. Wang, T. Shi and H. Zhang, *Chem. Commun.*, 2019, **55**, 12376–12379.

11 Y. Wang, J. Wang, H. Li, Y. Li, J. Li, K. Wei, F. Peng and F. Gao, *Small Struct.*, 2023, **4**, 2200306.